FACTA UNIVERSITATIS
Series: **Mechanical Engineering**
https://doi.org/10.22190/FUME240203027A

Original scientific paper

NOVEL SMART DESIGN OF REAR HALF SHAFT OF LARGE URBAN TRANSPORT VEHICLE

Fabio Alberti[1], Danilo D'Andrea[2], Alarico Macor[3], Giacomo Risitano[2], Antonio Rossetti[4], Aleksandar Sedmak[5,6]

[1]Department of Mechanical and Aerospace Engineering, Politecnico di Torino, Italy
[2]Department of Engineering, University of Messina, Italy
[3]Department of Engineering and Management, University of Padua, Italy
[4]Istituto per la Tecnologia della Costruzione, Consiglio Nazionale delle Ricerche, Italy
[5]Faculty of Mechanical Engineering, University of Belgrade, Serbia
[6]University of Brasov, Faculty of Civil Engineering, Brasov, Romania

Abstract. *New design method of rear half shaft of a large urban transport vehicle with a conventional (Power Shift) and hydro-mechanical (Power Split) transmission is presented. The so-called Smart Design is based on the automatic cumulative fatigue damage determination combining the Rainflow method and Palmgren-Miner rule. Previous study, comparing the Power Shift transmission with other alternatives, clearly demonstrated that the Power Split transmission offers significant advantages in terms of pollutant emissions and fuel consumption, making it a better choice for the ecological transition. Anyhow, from a mechanical point of view, the results of this work show that the load condition of the hydro-mechanical Power Split transmission reduce significantly the fatigue life of a component initially designed for a conventional transmission.*

Key words: *Large urban transport vehicle, Power Split/Shift transmission, Smart design, Cumulative fatigue damage*

1. INTRODUCTION

Problems of air pollution and road traffic noise are two important environmental troubles that could be harmful to the health and well-being of urban populations [1–3]. Many studies have been conducted focusing on the design of new type of transmission for high power density vehicles such as wheel loader [4] buses for urban transport [5], taxies [6,7] and other urban vehicles [8], to improve the efficiency of the system and reduce consumptions and emissions. In recent years, electric vehicles have been introduced, which have the potential

Received: February 03, 2024 / Accepted May 15, 2024
Corresponding author: Aleksandar Sedmak
Faculty of Mechanical Engineering, University of Belgrade, Kraljice Marije 16, 11000 Belgrade, Serbia
asedmak@mas.bg.ac.rs

to significantly reduce carbon emissions and improve air quality in urban areas, compared to conventional vehicles [9]. In addition, electric vehicles are generally quieter than internal combustion engine vehicles, which can help reduce noise pollution. This can be particularly beneficial for densely populated areas where noise pollution can have a significant impact on quality of life [10]. Despite the hybrid electric or full electric transmission is becoming more and more common in the automotive field, the costs and the reliability related to this technology make it unsuitable for all types of applications [11,12]. In this sense, the use of a hydro-mechanical transmission could be a valid solution attending for a more reliable and less expensive technology in the electric field. D'Andrea et al. [13] have compared a hydrostatic transmission with a hydro-mechanical transmission designed for an urban street sweeper, highlighting the advantage of using the hydro-mechanical transmission from the fuel consumption point of view. The same authors, have been investigated the fatigue damage of a front half shaft of a road car comparing three different fatigue damage criteria [14]. Related to a similar mechanical component, the drive axle housing of a truck was analyzed using static, fatigue, modal, harmonic response, and random vibration analyses [15]. Two lightweight optimization schemes were proposed: topology optimization, which reduced mass by 17.4%, and a multi-objective optimization approach. The latter approach achieved a reduction in mass of 4.35%, decreased equivalent stress by 21.05%, increased the minimum life of the component by 72.28%, and improved the natural frequencies. Asi [16] presents a failure analysis of a rear axle shaft from a car involved in an accident. The axle shaft was found to have fractured into two pieces. The purpose of the investigation was to determine whether the failure was the cause or a consequence of the accident. Various evaluation techniques were employed, including visual examination, photo documentation, chemical analysis, micro-hardness measurement, tensile testing, and metallographic examination. The results indicate that the axle shaft failed due to reversed bending fatigue caused by improper welding. Decker et al. [17] investigate the mechanics and interactions of wheel forces, suspension component forces, and axle casing stress in a multiaxial-randomly loaded air-suspension rear-axle for commercial vehicles. Fatigue, frequency, and correlation analyses are performed using load-time and stress-time data from a prototype vehicle tested on a track. The study identifies critical load situations affecting the axle's fatigue behavior under operational conditions, leading to optimized design solutions and experimental validation. Wu et al. [18] have investigated a hydro-mechanical continuously variable transmission for the all-terrain vehicle, evaluating the vehicle dynamic performance and the speed ratio control by simulation and experiment on a transmission prototype. Bayrakceken et al. [19] have been focused their study on the fracture analysis of a universal joint yoke and a drive shaft in the power transmission system of an automobile. The failures in these components can be attributed to various factors such as manufacturing and design faults, maintenance issues, raw material defects, material processing flaws, and user-related errors. Investigation involves spectroscopic and metallographic analyses, as well as hardness measurements for each part. Additionally, stress analyses using the finite element method are conducted to determine the stress conditions at the failed sections. Barone et al. [20] establish the T-N torsion fatigue curve at R = -1 for the front half-shaft mechanical system in an existing car. Experimental fatigue tests were conducted on 15 front half-shafts. Crack propagation evaluations and failure analysis were performed to identify the causes of the fractures. As a result, the T-N fatigue curve for the front half-shaft mechanical system was obtained.

By developing a multidisciplinary approach, it is possible to investigate the fatigue damage in mechanical components of the same vehicle equipped with different powertrain

solutions, ultimately aiming for an improved design. In this work, a comparison between the conventional transmission (Power Shift) and hydro mechanical transmission (Power Split) [21] of an urban bus has been carried out from both energetic and mechanical point of view. From the energetic point of view, a comparison between Power Shift and Power Split transmission has been already carried out by the authors in a previous work, highlighting the advantage of using Power Spilt transmission for the reduction of consumptions and emissions in urban buses [21]. In addition, the workflow adopted in this work has been already developed by the authors in a previous work [22] and it is indicated as "Smart Design". Smart Design consists of an automated and multi-object algorithm aimed at evaluate the fatigue damage of a mechanical component under specific load condition (e.g., Mission Test) for the best possible design, taking into account others design needs (e.g., environmental sustainability. The target component chosen for this work is the rear half shaft of an urban bus related to the traction. Through a cooperation between the University of Messina and the urban transport company ATM Messina S.p.A., it was possible to acquire different driving cycles in order to test both transmissions. The experimental setup consists of a portable control unit model SCADS XS compact provided by Siemens Company, together with a GPS and a tablet for monitoring the signals in real-time. Both Power Shift and Power Split transmission model have been developed in Simcenter Amesim™ environment. The models output of interest is the torque evaluated at the traction wheel, which represents the input load condition of the Finite Element Model (FEM) of the target component, developed in Ansys Workbench R2 2020™. The stress distribution evaluated from the FEM, has been used for evaluating the fatigue damage of the component, starting from the S-N curve of the material which the half shaft is made [23]. The automated algorithm developed in Matlab™ is based on the Rainflow method [24] and Goodman criterion [25]; the fatigue damage has been assessed by the Palmgren-Miner rule [26,27].

A key limitation in current methodologies is their inability to accurately model complex interactions in new powertrain technologies, especially under variable amplitude loading conditions. Previous studies have often failed to account for the nuanced effects of modern transmission systems on component stress and fatigue life, relying only on the energy efficiency of the vehicle without considering any mechanical aspects.

This study aims to address these gaps by introducing an enhanced analytical approach that combines advanced FEM analysis with the Goodman criterion for stress adjustment. By integrating these methodologies, a more accurate prediction of fatigue life under realistic operational conditions has been provided. Despite it was demonstrated that, with a proper management of the Internal Combustion Engine (ICE) in terms of torque and angular speed, the Power Split transmission turns out to be more energy efficient with respect to a traditional stepped gear transmission [5], it was remarked that the transmission change leads to a different fatigue damage, as shown in [22] by the comparison between a conventional and hybrid electric transmission. Also in this work, the results show that the Power Split transmission reduces the half shaft fatigue life in comparison to the Power Shift transmission, leading to the component failure. This approach allows for a more refined assessment of fatigue damage, particularly in automotive components subjected to complex load profiles. By surveying the drawbacks and limitations of previous studies, this research not only advances the theoretical framework but also significantly enhances practical applications in fatigue assessment.

2. MATERIALS AND METHODS

2.1 Reference Vehicle

The reference vehicle is a bus for urban transport. The transmissions topologies adopted in this work are the same already investigated by the authors in a previous work [21]. In particular, it was assessed that the adoption of a hydro mechanical Power Split transmission in urban buses leads to a reduction of fuel consumption with respect to conventional Power Shift transmission. The main geometric parameters of the bus are shown in Table 1.

2.2 Driving Cycle Acquisition

Different driving cycle of a typical route of the urban bus have been acquired in order to test both transmissions on a real Mission test. The driving cycles have been acquired in the city of Messina and the instrumentation used consisted of a portable control unit SCADS XS compact model, a GPS and a tablet, as already used in a previous work by the authors [22]. The GPS position of the vehicle extracted from Google Earth ™ are shown in Fig. 1, whereas Fig. 2 shows the acquired driving cycles.

Table 1 Geometrical and engine parameters of the reference vehicle

Parameter	Value
Vehicle model	Tector 7 Diesel Euro VI
Driving layout	Rear - Wheel Drive
Vehicle mass	19000 kg
Length	12 m
Height	3.066 m
Wheelbase	6.120 m
Maximum speed	Limited to 80 km/h
Engine	Tector 7 - EURO VI
Type	6 cylinders in - line, Common Rail
Engine volume	6.7 l
Maximum torque	1000 N at 1250-1700 rpm
Maximum power	210 kW at 2500 rpm

a) b) c) d)

Fig. 1 Driving cycles acquisition, GPS positions: (a) Cycle A, (b) Cycle B, (c) Cycle C, (d) Cycle D

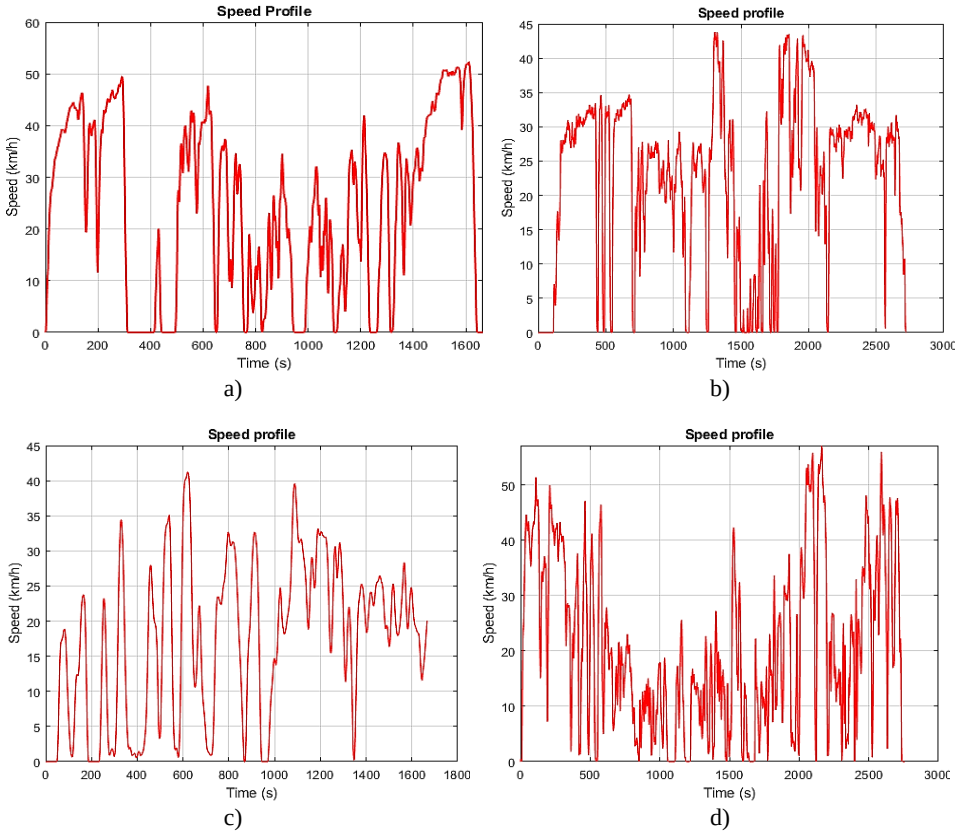

Fig. 2 Driving cycles acquisition, speed profile: a) Cycle A, b) Cycle B, c) Cycle C, d) Cycle D

2.3 Rear Half Shaft Finite Element Model (FEM)

The target component chosen for the cumulative fatigue damage calculation is the rear half shaft of the bus, which geometrical dimensions are shown in Fig. 3.

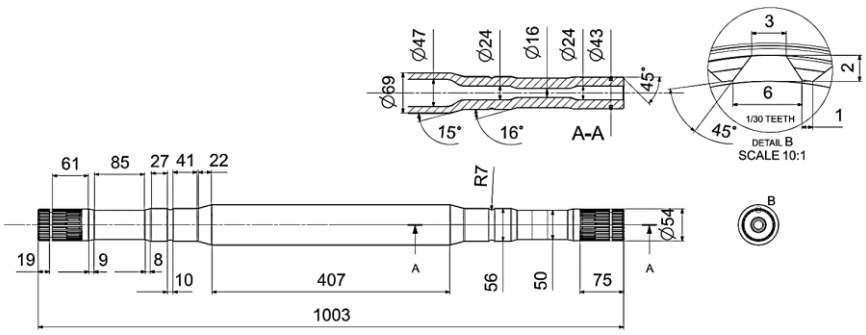

Fig. 3 Geometrical dimensions of the rear half shaft of the reference vehicle

The provided CAD of the shaft has been imported in SpaceClaim 2020 R2™, CAD extension of ANSYS Workbench 2020 R2™ software used for the FE simulations. In order to save computational time, it was possible to take advantage of the symmetry of the shaft simulating only one sector instead of the full shaft. Hence, three planes have been created: one orthogonal to the axis of symmetry of the shaft and two along the flank of the teeth. Then, through the Boolean operations, it was possible to cut the shaft along the planes direction as shown in Fig. 4a and Fig. 4b respectively.

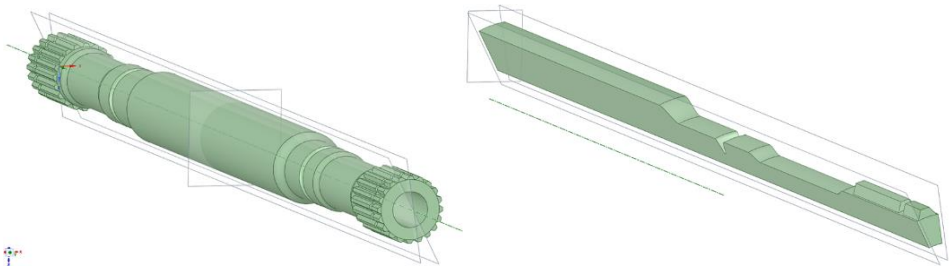

a) b)

Fig. 4 CAD geometry imported in SpaceClaim 2020 R2™ (a) Creation of the planes (b) Cutting of the geometry along the planes

2.4 Mesh Convergence

Before starting the FE simulations, it is necessary to perform a convergence analysis of the mesh through a static simulation. It is useful for choosing the right elements type and dimension in order to save computational time and maintain at the same time a good accuracy of the results. At the first, the cyclic region symmetry has been implemented, setting as Low boundary one flank of the teeth and High boundary the other. In addition, a local cylindrical reference system has been created on the geometry using the same rotation direction of the shaft. The mesh element type used in the FEM is a Tetra 3D element, which consist of a high order 20-node SOLID186 element with an initial dimension of 10 mm (Fig. 5a). In order to simulate the transmitted torque by the shaft, a spider beam (rigid connection) has been created on one flank of the teeth. This methodology allows simulating the force exchanged between the crown and the pinion, connecting all the nodes of the face to a remote point called Master Node (Fig. 5b). Then, all the boundary conditions have been settled. A fixed constrain has been inserted on one side of the shaft, locking all the displacements and rotations along the three axes. A cylindrical constrain has been inserted to the superior face of the shaft simulating a bearing support, locking the radial displacement and maintaining the axial and tangential displacement free. A static load of 1000 N (ramped) along x-axis, which is the exchanging force direction, has been associated to the remote point previously created (Fig. 5c). The simulation time has been settled to one second.

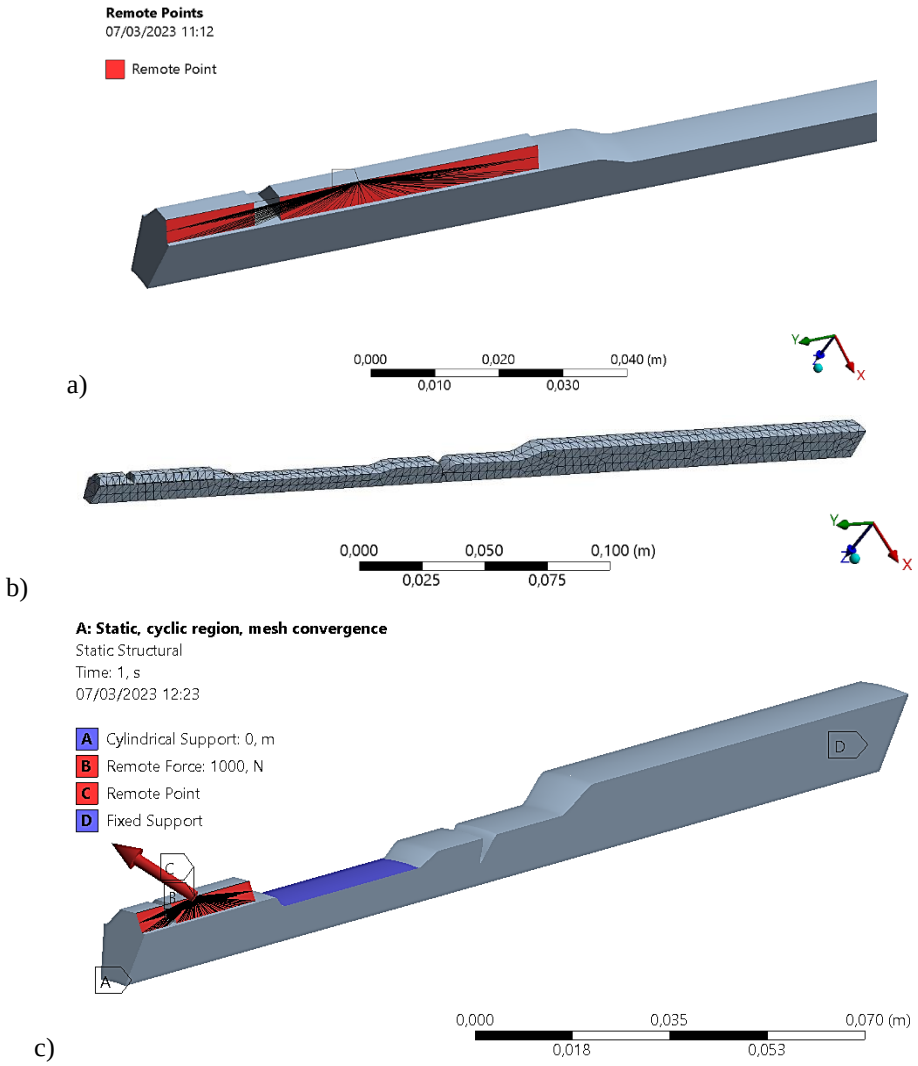

Fig. 5 Mesh convergence analysis through static simulation (a) Remote point creation (b) Mesh creation with an initial size of 10 mm (c) Load and constrain conditions

The results of the static simulation (total deformation) with the initial size of the mesh are shown in Fig. 6. The main advantage of the symmetry is that only one tooth can be modeled (Fig. 6a) instead of the full shaft (Fig. 6b), reducing the computational time.

Starting from the initial dimension of the mesh, different static simulations were performed reducing the mesh size, until the convergence of the total deformation value has been achieved (Fig. 7a). The optimal compromise between the accuracy of the results and the computational time has been obtained with a mesh size of 3 mm, confirmed also by a sensitivity analysis conducted varying the mesh size and recording the corresponding

deformation variation (Fig. 7b). The size of 3 mm was also adopted for the following fatigue analysis. The FEM model consist of 90429 nodes and 57515 elements.

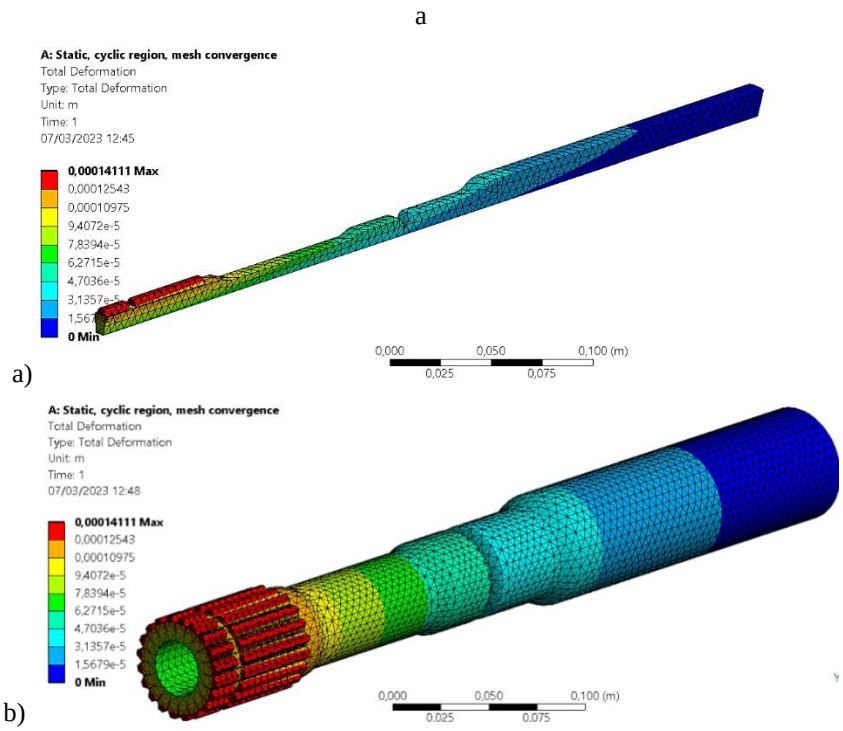

Fig. 6 Results of the static simulation - total deformation (a) One sector (b) Full shaft

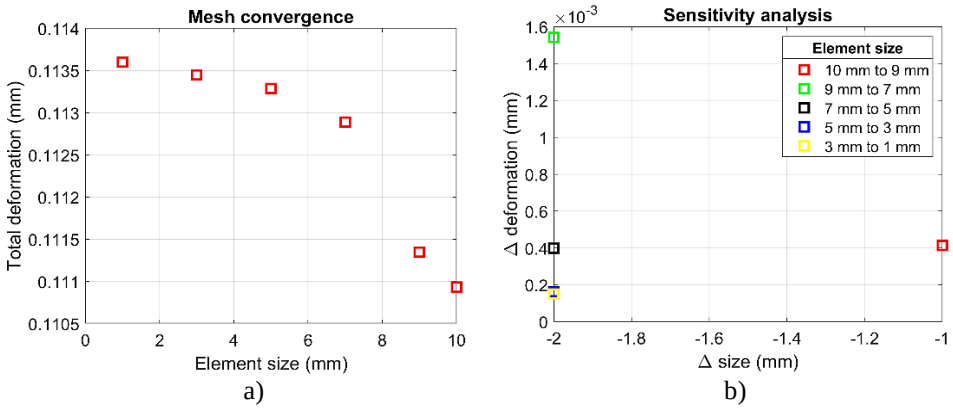

Fig. 7 Results of mesh convergence, (a) Total deformation value (b) Sensitivity analysis

2.5 Transient Simulation

With respect to the static simulation, in order to consider a variable load, it is necessary to perform a transient simulation. In this case, the FE software package does not allows taking advantage of the symmetry of the shaft using the symmetry cyclic region. Hence, the entire shaft has been investigated, using as load condition the torque values evaluated from Amesim^{TM} software for both Power Shift and Power Split transmission (Fig. 8).

Among the acquired driving cycles shown in Fig. 2, cycle A has been chosen as case study for testing the design method, since: i) it more accurately represents the typical or most demanding operating conditions that the vehicle or component experiences, including factors like average speed and typical load conditions; ii) the quality of the data collected during cycle A have been higher or more consistent compared to the other cycles, probably attributed to fewer data anomalies or more stable testing conditions during the data collection; iii) Cycle A covers a broader range of operating scenarios like urban and extra-urban run, providing a more comprehensive assessment of the component's performance across different stress levels and operational environments. As a consequence, the choice of cycle A align more closely with the specific research objectives or hypotheses being tested.

Investigating both the speed profile and GPS position in Fig. 1 and Fig. 2, it is possible to observe that the driving cycle consist of a high-speed zone related to the run in extra urban areas and a mid-speed zone related to urban areas. The high-speed values are therefore reflected in high demanded torque. Considering that the material has been modelled as linear-elastic, the torque values are proportional to the maximum stress values computed from the FEM analysis. Hence, the low torque values do not influence the maximum stress neither the fatigue life of the component, if the stress values are below the fatigue limit of the material. Taking into account these considerations, in order to save computational time only the first 300 s of the driving cycle have been considered.

The boundary conditions are the same of the static simulation (Fig. 5c) as well as the mesh size, with the difference that the torque (moment) is directly applied to all the flank of the teeth as shown in Fig. 9.

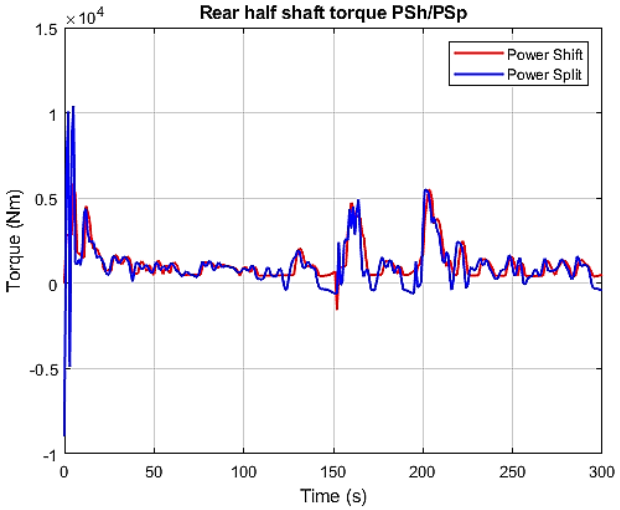

Fig. 8 Torque at the rear half shaft computed from AmesimTM software

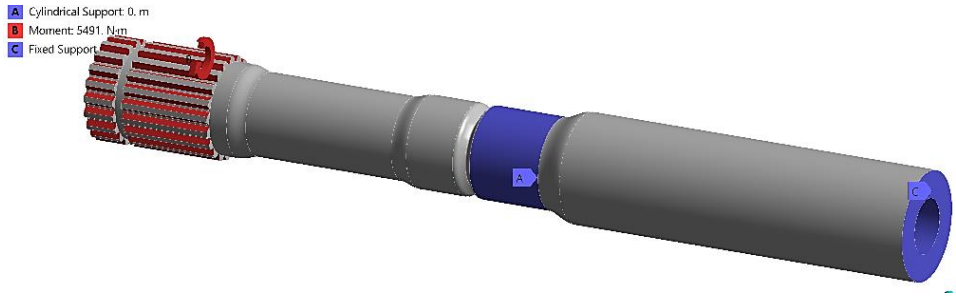

Fig. 9 Load and constrain conditions applied to the transient simulation

2.5 Smart Design Algorithm

The Smart Design algorithm represents a novel, rapid, and automated methodology proposed by the authors to assess fatigue damage in mechanical components and to optimize their design through multi-objective analysis. With respect to the previous work by the authors [22], the input data of the algorithms is the stress distribution evaluated from the FEM (fatigue analysis). At the first, it is necessary the knowledge of the fatigue behavior of the material through experimental tests. The material of which the half shaft is made is the AISI 4130 steel (25CrMo4 according to ISO 683-18, EN 10083-1 standard), typically used for the production of shaft in heavy vehicles [28]. The mechanical properties, as well as the chemical composition of the employed material are shown in Table 2 [20].

Table 2 Mechanical properties and chemical composition of AISI 4130 steel [20]

Parameter	Value
Tensile strength	670 MPa
Yield strength	435 MPa
Carbon (C) %	0.28 ÷ 0.33
Chromium (Cr) %	0.80 ÷ 1.10
Molybdenum (Mo) %	0.15 ÷ 0.25
Manganese (Mn) %	0.40 ÷ 0.60
Silicon (Si) %	0.15 ÷ 0.35
Phosphorus (P) %	0.035
Sulfur (S) %	< 0.04

The S-N curve of the material has been obtained from a literature study [23] in which the authors have been conducted tensile fatigue test on regulated specimen with a load ratio R = -1. The experimental results have been then fitted with the Basquin equation [29,30] according to Eq. (1):

$$\sigma_a = \mathrm{A} N_f^{\mathrm{b}} \tag{1}$$

where σ_a is the stress amplitude, N_f are the failure cycles, A and b are two regression constants. Fig. 10a and Fig. 10b show the specimen geometry and the S-N curve with Basquin equation obtained from experimental fatigue tests respectively [23].

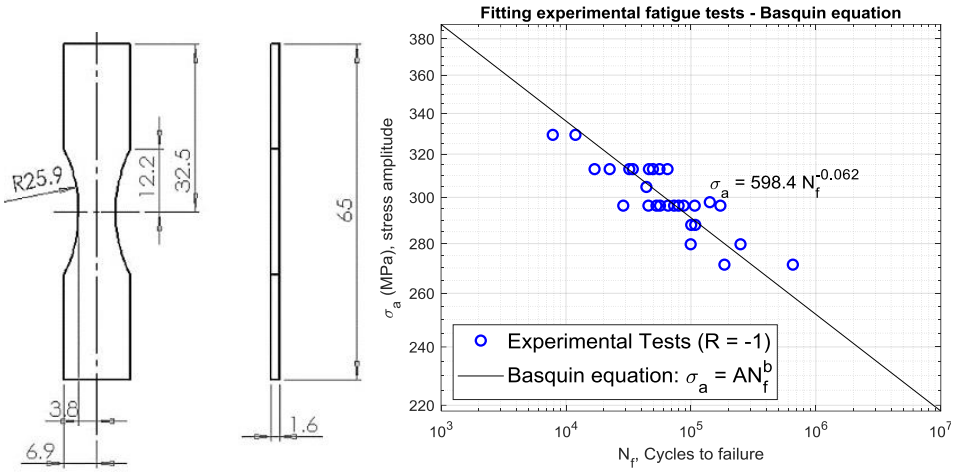

Fig. 10 Fatigue tensile tests, [23], (a) Geometry of the specimens (b) S-N curve

The stress distribution evaluated from the numerical simulation derives from a random load in the time domain. Therefore, it is necessary to extrapolate an equivalent stress distribution referred at R = -1, in order to evaluate the fatigue damage from the S-N curve of the material (Fig. 10b). At the first, the driving cycle has been repeated until the design target is reached, in this work, 800000 km. Then, the Rainflow method [24] has been applied. The Rainflow method is a fatigue analysis technique that decomposes complex variable amplitude load histories into simple, reversible stress cycles. It identifies and counts these cycles by analyzing peaks, troughs, and reversals in the load spectrum, which are critical for assessing the fatigue life of a component. This method allows for the precise calculation of fatigue damage by correlating these cycles with the material's S-N curve. Hence, the obtained load histories are characterized by a certain stress range σ_a, stress mean σ_m, number of working cycle N and load ratio R which, in the vast majority of cases, turns out to be different to R = -1. In order to convert all the load histories into an equivalent one at R = -1, the Goodman criterion [25] has been applied, as in Eq. (2)

$$\frac{\sigma_a}{\sigma_{ar}} + \frac{\sigma_m}{\sigma_u} = 1 \tag{2}$$

where σ_a is the stress range computed from the Rainflow method, σ_{ar} is the equivalent stress range referred to R = -1, σ_m is the stress mean and σ_u is the ultimate strength. Following the application of the Goodman criterion, the load histories are characterized by specific numbers of working cycles at R = -1. These adjusted load histories are then intersected with the fitting line of the experimental data, evaluated according to Eq. (1), to derive the number of failure cycles, which are subsequently used in calculating fatigue damage. The fatigue damage has been measured applying the Palmgren – Miner rule [26,27], defined by Eq. (3):

$$\sum_i \frac{n_i}{N_i} \tag{3}$$

where n_i is the number of working cycles and N_i the number of failure cycles.

3. Results and Discussions

The transmission models developed in Amesim™ environment have been validated comparing the speed profile of both transmissions with the imposed one (mission test). The control system acts as follow:

- Power shift transmission. The transmission in controlled by a rotary friction placed after the differential gear (final drive). The rotary friction controls the amount of torque necessary to follow the speed profile acting as a brake (friction torque) when it is open or partially open.
- Power Split transmission. The transmission is controlled by the swash plate angle of the hydraulic pump. More is the swash plate angle more is the oil flow rate inside the hydraulic circuit used to accelerate the vehicle.

The quality of the control system is reflected in a near-perfect adhesion between the mission test and the speed profiles of both transmissions as shown in Fig. 11.

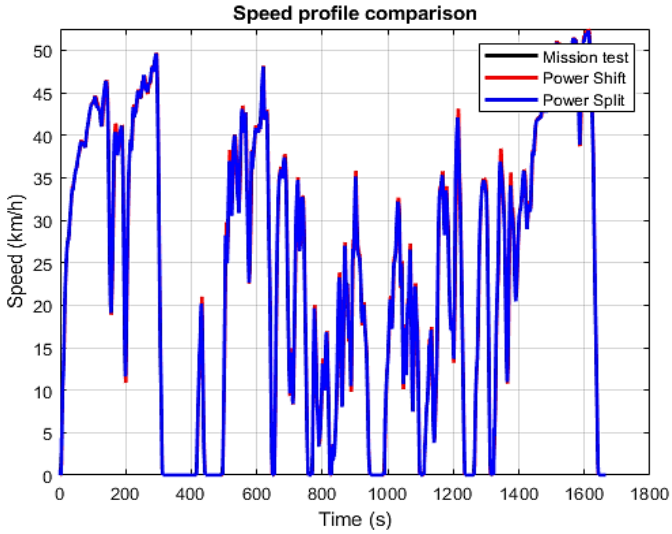

Fig. 11 Comparison between the mission test and the speed profiles of Power Shift and Power Split transmission

The results of the transient simulation are shown in Fig. 12a and Fig. 12b in which the equivalent stress (Von-Mises) has been compared for both Power Shift and Power Split transmission.

From the investigation of Fig. 12 is possible to assert that, despite the torque levels are quite similar for both transmission (Fig. 8), the Power Split transmission presents a higher stress distribution, especially in the first part of the driving cycle, as also shown in Fig. 13.

The maximum stress values are recorded in the restricted sections and junctions, as expected from the fatigue theory about the stress concentration, with a peak value of 2000 MPa for the Power Split transmission and 1300 MPa for the Power Shift transmission. The Rainflow method has been applied to both stress distributions. The Rainflow histograms regarding the Power Shift and Power Split transmissions are shown in Fig. 14a and Fig. 14b, respectively.

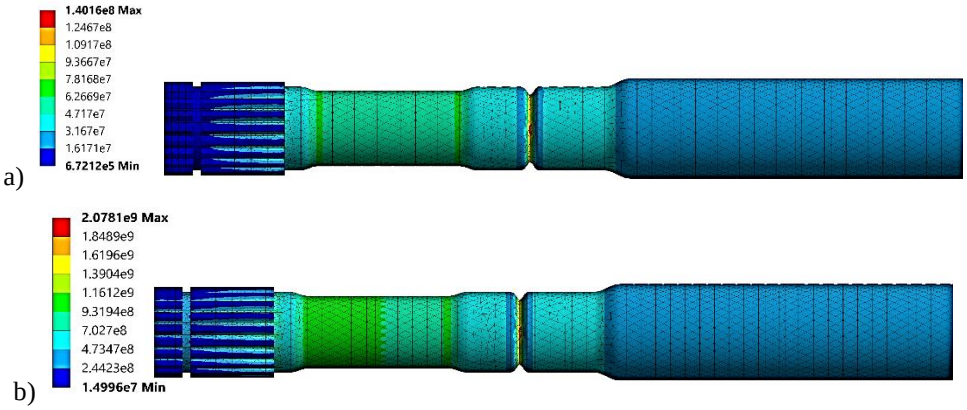

Fig. 12 Results of the transient simulation in terms of equivalent stress (Von Mises) Power Shift (b) Power Split

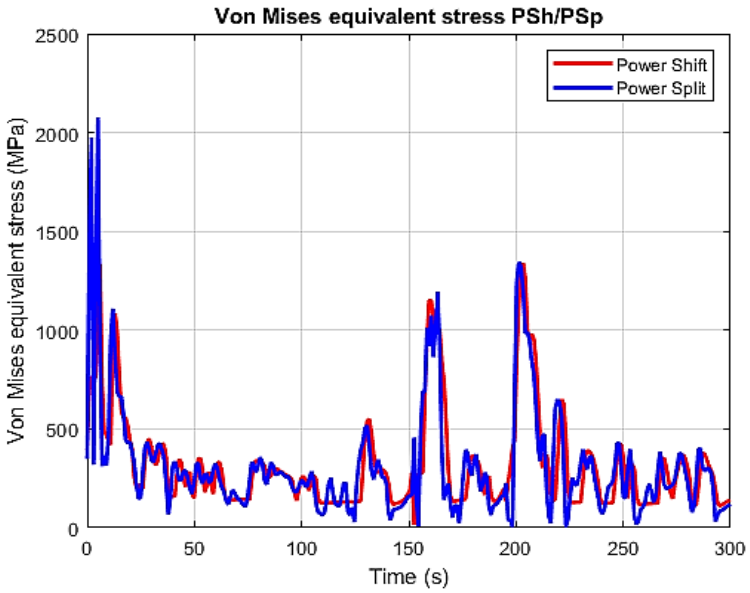

Fig. 13 Von Mises equivalent stress comparison between Power Shift and Power Split

At the end, all the stress cycles have been referred to a load ratio R = -1 through the Goodman criterion expressed in Eq. (2). Through the Smart Design algorithm, it was possible to calculate the fatigue damage on the component by applying the Miner rule expressed in (3). Stress cycles below the fatigue limit of the material does not contribute to the fatigue damage calculation while, for every stress cycle above the fatigue limit, the working cycles n_i and the failure cycles N_i have been calculated respectively. The stress cycles for the Power Shift and Power Split transmission are shown in Fig. 15.

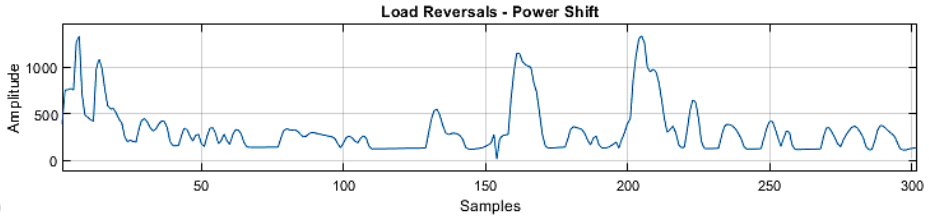

a)

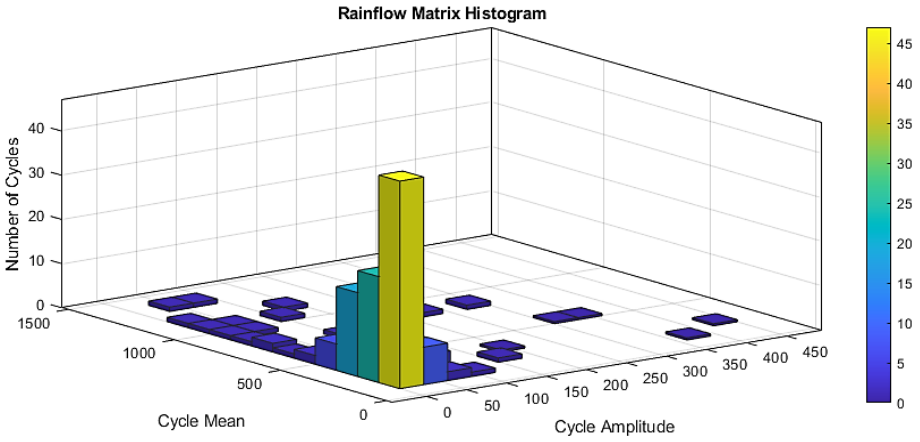

b)

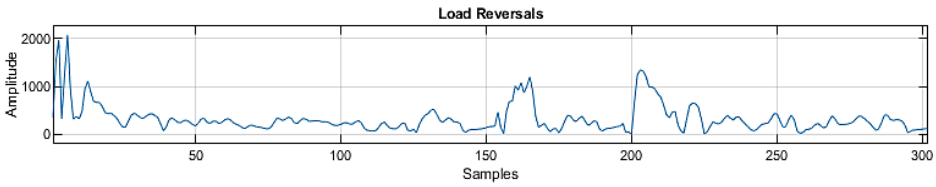

c)

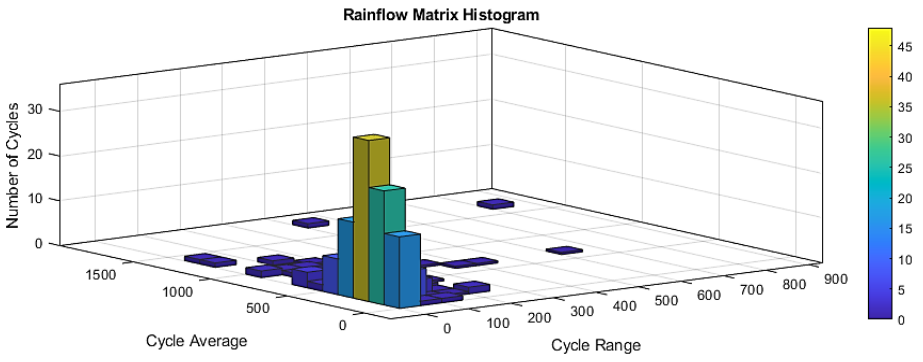

d)

Fig. 14 Rainflow method results: a) cycle amplitude - Power Shift, b) cycle mean - Power Shift, c) cycle amplitude - Power Split, b) cycle mean - Power Split

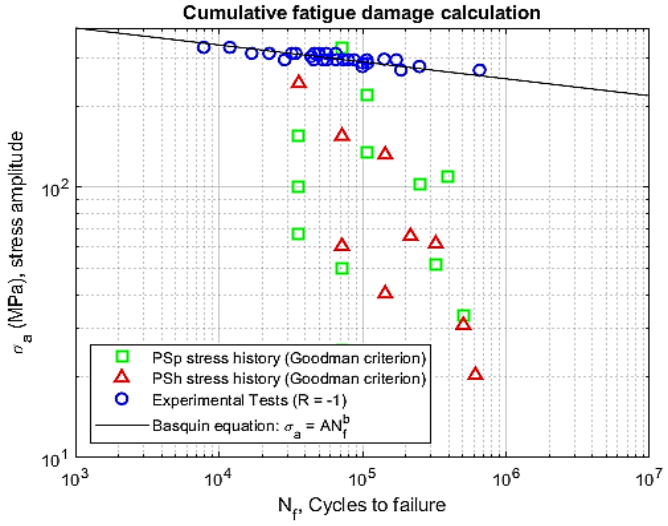

Fig. 15 Equivalent stress cycles referred to a load ratio R = -1. Comparison between Power Split (green) and Power Shift (red) transmission

The measured fatigue damage for Power Shift transmission is:

$$\sum_i \frac{n_{i\,PSh}}{N_{i\,PSh}} = \frac{36000}{3.5 \cdot 10^6} \approx 0.01 \approx 1\% \tag{4}$$

As can be observed from Fig. 15, one load history related to the Power Split transmission (labeled as PSp and green square in the figure) exceeds the S-N curve. This indicates that this load history causes the failure of the component, particularly occurring at ~300 MPa and 72000 cycles.

4. CONCLUSIONS

In this study, a multidisciplinary approach has been adopted to assess the fatigue damage of the rear half shaft in an urban bus, focusing on two transmission types: Power Shift and Power Split. The findings of the work reveal that, although the Power Split transmission offers substantial environmental benefits by reducing fuel consumption and emissions, it introduces significant mechanical challenges due to the integration of the hydraulic branch. Specifically, the Power Split transmission was found to exacerbate fatigue damage compared to the Power Shift transmission, thereby reducing the component's lifespan. This critical insight necessitates the redesign or adaptation of components to withstand the load profiles imposed to the Power Split transmission, while maintaining fatigue resistance. Consequently, the research provides a vital foundation for further studies and design optimizations, which are essential to advance sustainable propulsion systems without compromising mechanical reliability. Future work should focus on developing and testing components that can endure the demands of Power Split transmissions. Additionally, collaborations with vehicle manufacturers to apply these findings in real-world settings would be instrumental in refining the design of sustainable,

robust mechanical systems for urban buses. In conclusion, while the environmental advantages of the Power Split transmission are clear, ensuring the mechanical integrity and longevity of components in such systems is paramount. The study underscores the need for a careful consideration of mechanical implications when deploying new propulsion technologies and highlights the path forward for enhancing both the efficiency and reliability of transportation technologies.

REFERENCE

1. Apparicio, P., Gelb, J., Carrier, M., Mathieu, M.È., Kingham, S., 2018, *Exposure to noise and air pollution by mode of transportation during rush hours in Montreal*, J Transp Geogr, 70, pp. 182–92.
2. Reis, S, Cowie, H., Riddell, K., Steinle, S., Apsley, A., 2013, Urban air quality citizen science Phase 1 : Review of methods and projects.
3. Kim, M., Chang, S.I., Seong, J.C., Holt, J.B., Park, T.H., Ko, J.H., Croft, J.B., 2012, *Road traffic noise*. Handb Highw Eng, 43(4), pp. 353-360.
4. Liu, X., Sun, D., Qin, D., Liu, J., 2017, *Achievement of fuel savings in wheel loader by applying hydrodynamic mechanical power split transmissions*, Energies, 10(9), 1267.
5. Rossetti, A., Macor, A., Benato, A., 2017, I*mpact of control strategies on the emissions in a city bus equipped with power-split transmission*, Transp Res Part D Transp Environ, 50, pp. 357–371.
6. Nyhan, M., Sobolevsky, S., Kang, C., Robinson, P., Corti, A., Szell, M., et al., 2016, *Predicting vehicular emissions in high spatial resolution using pervasively measured transportation data and microscopic emissions model*, Atmos Environ, 140, pp. 352–363.
7. Luo, X., Dong, L., Dou, Y., Zhang, N., Ren, J., Li, Y., et al., 2017, *Analysis on spatial-temporal features of taxis' emissions from big data informed travel patterns: a case of Shanghai, China*. J Clean Prod, 142, pp. 926–935.
8. Saboohi, Y., Farzaneh, H., 2009, *Model for developing an eco-driving strategy of a passenger vehicle based on the least fuel consumption*, Appl Energy, 86, pp. 1925–1932.
9. Sun, X., Li, Z., Wang, X., Li, C., 2020, *Technology Development of Electric Vehicles: A Review*, Energies, 13(1), 90.
10. Sanguesa, J.A., Torres-sanz, V., Garrido, P., Martinez, F.J., Marquez-barja, J.M., 2021, *A Review on Electric Vehicles : Technologies and Challenges*, Smart Cities, 4(1), pp. 372–404.
11. Pelletier, S., Jabali, O., Laporte, G., Veneroni. M., 2017, *Battery degradation and behaviour for electric vehicles : Review and numerical analyses of several models*, 103, pp. 158–187.
12. Almouhanna, A., Quintero-araujo, C.L., Panadero, J., Juan, A.A., Khosravi, B., Ouelhadj, D., 2020, *Computers and Operations Research The location routing problem using electric vehicles with constrained distance*. Comput Oper Res, 115, 104864.
13. Andrea, D.D., Risitano, G., Alberti, F., 2022, *Fuel Consumption Reduction and Efficiency Improvement in Urban Street Sweeper Using Power Split with Lockup Clutch Transmission*. Appl. Sci. 12(19), 10160
14. Alberti, F., Foti, P., Berto, F., Risitano, G., D'Andrea, D., 2022, *Fatigue life evaluation of automotive mechanical components by using smart design algorithm*, Fatigue Fract Eng Mater Struct, 46(4), pp. 1401–1412.
15. Zheng, B., Fu, S., Lei, J., 2022, *Topology Optimization and Multiobjective Optimization for Drive Axle Housing of a Rear Axle Drive Truck*, Materials, 15(15), 5268.
16. Asi, O., 2006, *Fatigue failure of a rear axle shaft of an automobile*, Eng Fail Anal, 13, pp. 1293–1302.
17. Decker, M., Savaidis, G., 2002, *Measurement and analysis of wheel loads for design and fatigue evaluation of vehicle chassis components*, Fatigue Fract Eng Mater Struct, 25, pp. 1103–1119.
18. Wu, W., Luo, J., Wei, C., Liu, H., Yuan, S., 2020, *Design and control of a hydro-mechanical transmission for all-terrain vehicle*, Mechanism and Machine Theory, 154, 104052,
19. Bayrakceken, H., Tasgetiren, S., Yavuz, I., 2007, *Two cases of failure in the power transmission system on vehicles: A universal joint yoke and a drive shaft*, Eng Fail Anal, 14, pp. 716–724.
20. Barone, C., Casati, R., Dusini, L., Gerbino, F., Guglielmino, E., Risitano, G., et al., 2018, *Fatigue life evaluation of car front halfshaft*. Procedia Struct Integr, 12, pp. 3–8.
21. MacOr, A., Rossetti, A., 2013, *Fuel consumption reduction in urban buses by using power split transmissions*. Energy Convers Manag, 71, pp. 159–171.

22. Previti, U., Galvagno, A., Risitano, G., Alberti, F., 2022, *Smart Design: Application of an Automatic New Methodology for the Energy Assessment and Redesign of Hybrid Electric Vehicle Mechanical Components.* Vehicles, 4, pp. 586–607.
23. Singh, K., Sadeghi, F., Correns, M., Blass, T., 2019, *A microstructure based approach to model effects of surface roughness on tensile fatigue*, Int J Fatigue, 129, 105229.
24. Marsh, G., Wignal, C., Thies, P.R., Barltrop, N., Incecik, A., Venugopal, V., Johanning, L., 2016, *Review and application of Rainflow residue processing technique for accurate fatigue damage estimation*, Int J Fatigue, 82, pp. 757–765.
25. Gujar, R.A., Bhaskar S.V., 2013, *Shaft design under fatigue loading by using modified Goodman criterion*, IJERA, 3, pp. 1061-1066.
26. Dikmen, F., Bayraktar, M., Guclu, R., 2012, *Railway axle analyses: Fatigue damage and life analysis of rail vehicle axle*. Stroj Vestnik/Journal Mech Eng, 58, pp. 545–552.
27. Weber, F., Wu, H., Starke, P., 2023, *A new short-time procedure for fatigue life evaluation based on linear damage accumulation by Palmgren-Miner*, Int J Fatigue, 172, 107653.
28. Duffner, D.H., 2006, *Torsion fatigue failure of bus drive shafts*, J Fail Anal Prev, 6, pp. 75–82.
29. Starke, P., Walther, F., Eifler, D., 2009, *New fatigue life calculation method for quenched and tempered steel SAE 4140*, Mater Sci Eng A, 523, pp. 246–252.
30. Niesłony, A., Dsoki, C., Kaufmann, H, Krug, P., 2008, *New method for evaluation of the Manson-Coffin-Basquin and Ramberg-Osgood equations with respect to compatibility*, Int J Fatigue, 30, pp. 1967–1977.